Visualizing gene expression by whole-body fluorescence imaging

Meng Yang*, Eugene Baranov*, A. R. Moossa†, Sheldon Penman‡, and Robert M. Hoffman*†§

*AntiCancer, Inc., 7917 Ostrow Street, San Diego, CA 92111; †Department of Surgery, University of California, 200 West Arbor Drive, San Diego, CA 92103-8220; and ‡Department of Biology, Massachusetts Institute of Technology, 77 Massachusetts Avenue, Cambridge, MA 02139-4307

Contributed by Sheldon Penman, August 14, 2000

Transgene expression in intact animals now can be visualized by noninvasive techniques. However, the instruments and protocols developed so far have been formidable and expensive. We describe here a system for rapidly visualizing transgene expression in major organs of intact live mice that is simple, rapid, and eminently affordable. Green fluorescent protein (GFP) is expressed in the cells of brain, liver, pancreas, prostate, and bone, and its fluorescence is encoded in whole-body optical images. For low-magnification images, animals are illuminated atop a fluorescence light box and directly viewed with a thermoelectrically cooled color charge-coupled device camera. Higher-magnification images are made with the camera focused through an epi-fluorescence dissecting microscope. Both nude and normal mice were labeled by directly injecting 8×10^{10} plaque-forming units/ml of adenoviral GFP in 20–100 μl PBS and 10% glycerol into either the brain, liver, pancreas, prostate, or bone marrow. Within 5–8 h after adenoviral GFP injection, the fluorescence of the expressed GFP in brain and liver became visible, and whole-body images were recorded at video rates. The GFP fluorescence continued to increase for at least 12 h and remained detectable in liver for up to 4 months. The system's rapidity of image acquisition makes it capable of real-time recording. It requires neither exogenous contrast agents, radioactive substrates, nor long processing times. The method requires only that the expressed gene or promoter be fused or operatively linked to GFP. A comparatively modest investment allows the study of the therapeutic and diagnostic potential of suitably tagged genes in relatively opaque organisms.

green fluorescent protein fluorescence optical imaging | *in vivo* gene expression | real time

Gene expression, when studied in cultured animal cells, is largely concerned with scalar quantities such as the amount of gene product. Extending these studies to the expression of genes in whole animals adds spatial and temporal dimensions. The regional distribution of gene activity is of fundamental importance as is the timing of response to physiological signals. Making such measurements in animals has been extremely difficult. Every data point required killing and dissecting the experimental animal and measuring the distribution of a reporter gene. Following a time course in a single subject was, of course, impossible.

New techniques can visualize transgene expression noninvasively in intact animals and promise a veritable revolution in genetic and physiological studies (1–6). The methods are a significant extension of the century-old, noninvasive imaging of the internal tissues of intact animals. From Röntgen's x-rays to modern computed x-ray tomography and MRI, the static distribution of tissue mass has been visualized with ever-increasing resolution. Recent developments, such as MRI, have made possible visualizing dynamic processes. Now, noninvasive imaging has been extended to imaging the spatial distribution of transgene expression in living animals. Marker gene products have been visualized by MRI (2–3), by emitted gamma rays in micropositron emission tomography (4) and single-photon emission computed tomography (5), or by luciferin fluorescence (6). Unfortunately, the procedures require complex and expensive apparatus as well as the administration either of contrast agents or substrates that are radioactive or fluorescent. Also, the signals are generally weak and so require long processing times, which limits detailed time-course measurements.

This report describes a simple, inexpensive optical system using GFP as a reporter. It can visualize gene expression in small mammals requiring only that the gene under study be coupled to GFP. The measurements are sufficiently rapid as to allow video recording for real-time measurements. The apparatus is sufficiently modest as to allow many laboratories to adopt the technique.

Materials and Methods

Animals. Four- to 6-week-old both male and female nude/nude, nude/+, and C57BL/6 mice were used. All animal studies were conducted in accordance with the principles and procedures outlined in the National Institutes of Health Guide for the Care and Use of Animals under assurance number A3873–1. Mice were fed with autoclaved laboratory rodent diet (Tecklad LM-485, Western Research Products, Orange, CA).

DNA Expression Vector. The adenoviral (vAd) vector AdCMV5GFPAE1/AE3 [vAd-green fluorescent protein (GFP)] (Quantum, Montreal, Canada) expresses enhanced GFP and the ampicillin resistance gene.

Delivery of vAd-GFP to Various Organs. *Brain*. The parietal bone of the skull was exposed after an upper midline scalp incision. Twenty microliters containing 8×10^{10} plaque-forming units (pfu)/ml vAd-GFP per mouse was injected in the brain by using a 1-ml 27G1/2 latex-free syringe (Becton Dickinson). The puncture hole in the skull was plugged with bone wax. The incision in the scalp was closed with a 7–0 surgical suture in one layer. The animals were kept under isofluorane anesthesia during surgery.

Liver. The portal vein was exposed after an upper midline abdominal incision. One-hundred microliters containing 8×10^{10} pfu/ml vAd-GFP per mouse was injected in the portal vein by using a 1-ml 30G½ latex-free syringe (Becton Dickinson). The puncture hole in the portal vein was pressed for about 10 sec with sterile cotton for hemostasis. The incision in the abdominal wall was closed with a 7–0 surgical suture in one layer. The animals were kept under Ketsel anesthesia during surgery. All procedures of the operation described above were performed with a ×7 magnification stereo microscope (Leica MZ12, Nussloch, Germany).

Abbreviations: GFP, green fluorescent protein; vAd, adenoviral; pfu, plaque-forming unit.

§To whom reprint requests should be addressed at: AntiCancer, Inc., 7917 Ostrow Street, San Diego, CA 92111. E-mail: all@anticancer.com.

The publication costs of this article were defrayed in part by page charge payment. This article must therefore be hereby marked "*advertisement*" in accordance with 18 U.S.C. §1734 solely to indicate this fact.

Pancreas. The pancreas was exposed after an upper midline abdominal incision. One-hundred microliters containing 8×10^{10} pfu/ml vAd-GFP per mouse was injected in the pancreas by using a 1-ml 30G½ latex-free syringe (Becton Dickinson). The puncture hole was pressed for about 10 sec with sterile cotton for hemostasis. The incision was closed with a 7–0 surgical suture in one layer. The animals were kept under Ketsel anesthesia during surgery. All procedures of the operation described above were performed with a ×7 magnification stereo microscope.

Prostate. The bladder and prostate were exposed after a lower midline abdominal incision. Thirty microliters containing 8×10^{10} pfu/ml vAd-GFP per mouse was injected in the prostate by using a 1-ml 30G½ latex-free syringe (Becton Dickinson). The puncture hole in the prostate was pressed for about 10 sec with sterile cotton for hemostasis. The incision in the abdominal wall was closed with a 6–0 surgical suture in one layer. The animals were kept under isoflurane anesthesia during surgery. All procedures of the operation described above were performed with a ×7 magnification stereo microscope.

Bone Marrow. For bone marrow injection, animals were anesthetized by inhalation of isofluorane. The skin on the hind leg was opened with a 1-cm incision to expose the tibia. A 27-gauge needle with latex-free syringe (Becton Dickinson) then was inserted in the bone marrow cavity. A total volume of 20 μl (8×10^{10} pfu/ml) vAd-GFP per mouse was injected into the bone marrow cavity. The puncture hole in the bone was plugged with bone wax, and the incision was closed with a 6–0 surgical suture.

External Imaging of Transgene Expression. A Leica fluorescence stereo microscope, model LZ12, equipped with a 50-W mercury lamp, was used for high-magnification imaging. Selective excitation of GFP was produced through a D425/60 band-pass filter and 470 DCXR dichroic mirror. Emitted fluorescence was collected through a long-pass filter GG475 (Chroma Technology, Brattleboro, VT) on a Hamamatsu C5810 3-chip cooled color charge-coupled device camera (Hamamatsu Photonics Systems, Bridgewater, NJ). Images were processed for contrast and brightness and analyzed with the use of IMAGE PRO PLUS 3.1 software (Media Cybernetics, Silver Springs, MD). Images of 1,024 × 724 pixels were captured directly on an IBM PC or continuously through video output on a high-resolution Sony VCR model SLV-R1000 (Sony, Tokyo). Imaging at lower magnification that visualized the entire animal was carried out in a light box illuminated by blue light fiber optics (Lightools Research, Encinitas, CA) and imaged by using the thermoelectrically cooled color charge-coupled device camera, as described above.

Measuring the Intensity of GFP Expression. Estimating the intensity of GFP fluorescence is complicated by variations in the exciting illumination with time and across the imaging area. These factors are corrected for by using the intrinsic red fluorescence of mouse skin as a base line to correct the increase over intrinsic green fluorescence caused by GFP. This can be done because there is relatively little red luminance in the GFP radiance. Consequently, the green fluorescence was calculated relatively to red based on red and green channel composition in the skin image. A ratio (γ) of green to red channels was determined for each pixel in the image of skin without and with GFP. Values of γ for mouse skin throughout the image in the absence of GFP were fairly constant, varying between 0.7 and 1.0. The contribution of GFP fluorescence from within the animal increased the green component relative to red, which was reflected in higher γ values. The total amount of GFP fluorescence was approximated by multiplying the number of pixels in which value γ was higher than 1 times the γ value of each pixel. Such a product roughly corresponds to the integral GFP fluorescence $[I'_{GFP}]$ above the maximum value of γ for skin without GFP. The number of pixels in mouse skin images with γ value > 1.0 without GFP was less than 0.02% and increased with GFP expression. The value of $[I'_{GFP}]$ is presented as a function of time after virus injection in Figs. 3 and 5 for the brain and liver.

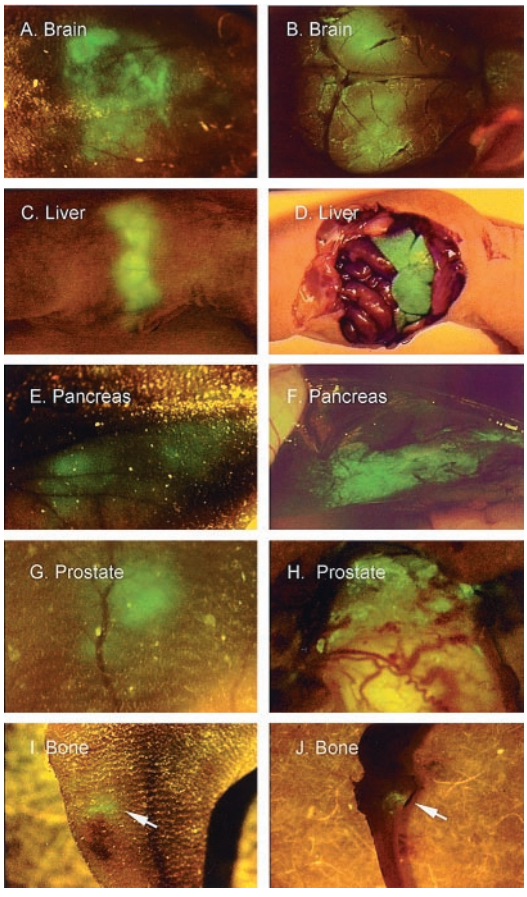

Fig. 1. External and internal images of vAd-GFP gene expression in various organs. External fluorescent whole-body images were compared with direct images of vAd-GFP gene expression in various organs. Series of external fluorescence images of vAd-GFP gene expression in brain, liver, pancreas, prostate, and tibia, (*A*, *C*, *E*, *G*, and *I*) compared with corresponding images of the exposed organs (*B*, *D*, *F*, *H*, and *J*). See *Materials and Methods* for vector delivery and imaging details.

Results

Fluorescence of vAd-GFP Gene Expression in Labeled Mouse Organs. The crucial test of external imaging is its ability to represent the internal distribution of gene activity. Fig. 1 compares external images of vAd-GFP fluorescence from labeled mouse organs in live, intact animals to the fluorescence of the organs viewed directly after death and dissection. The fluorescence maps the region of gene expression in the brain (Fig. 1 *A* and *B*), liver (Fig. 1 *C* and *D*), pancreas (Fig. 1 *E* and *F*), prostate (Fig. 1 *G* and *H*), and bone (Fig. 1 *I* and *J*). The images made externally to the animal appear very similar to those of the exposed organs, reproducing much of the detailed structure of the direct image.

Real-Time Quantitative Whole-Body Imaging of vAd-GFP Gene Expression. Another important advantage of the GFP fluorescence assay for gene expression is its extremely rapid data acquisition. Under the conditions used here, images could be obtained at video rates, i.e., with exposure times in the order of 1/30 sec. The fluorescence from vAd-GFP gene expression in the brain of a single animal was visible within 6 h after local delivery of the

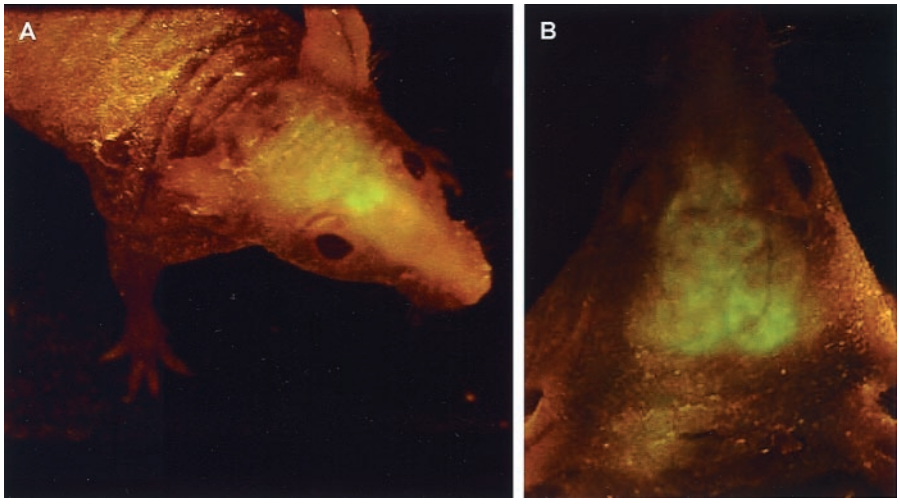

Fig. 2. External whole-body image of vAd-GFP gene expression in the brain. An external image of vAd-GFP gene expression in the brain acquired from a nude mouse in the light box 24 h after gene delivery. Clear image of transgene expression in the brain can be visualized through the scalp and skull. See *Materials and Methods* for imaging.

vAd-GFP gene in a nude mouse (Fig. 2). The fluorescence intensity was monitored by real-time video recording and measured as described in *Materials and Methods*. The data are shown in Fig. 3. Liver fluorescence first became detectable at about 7 h after the injection of vAd-GFP into the tail vein. The time course of observed intensity measured from a video recording is plotted in Fig. 4.

Whole-Body, External Images of vAd-GFP Gene Expression in Liver. The simplest and most rapid method of observing whole-body fluorescent images of vAd-GFP gene expression is shown in Fig. 5. Images showing fluorescence emanating from the liver were acquired from a mouse freely moving in a light box (Fig. 5). This inexpensive system suggests the feasibility of high-throughput screening of agents that affect specific gene expression.

Imaging Sensitivity. GFP transgene expression in various organs and tissues was considered to be externally measurable if the average fluorescence of the GFP-expressing organs was at least 20% above the average fluorescence of the surrounding skin. The fluorescence intensity at maximal level of GFP expression in the liver exceeded more than 100 times backdorsal and abdominal skin fluorescence. The intensity of GFP fluorescence of vAd-GFP expression in the mouse liver at a depth of 0.8 mm under the skin was ≈25% of that of the exposed organ.

Discussion

The enormous potential of visualizing gene expression in intact living animals has motivated development of several quite ingenious techniques. MRI is a nonoptical method that has been adapted for imaging a transgene product that perturbs the magnetic field. MRI can image intact, opaque organisms in three dimensions with resolution at approximately 50 μM^3 (2). However, the low sensitivity entails long imaging times and consequently slow data acquisition. Most importantly, the method depends on administering a systemic contrast agent selectively

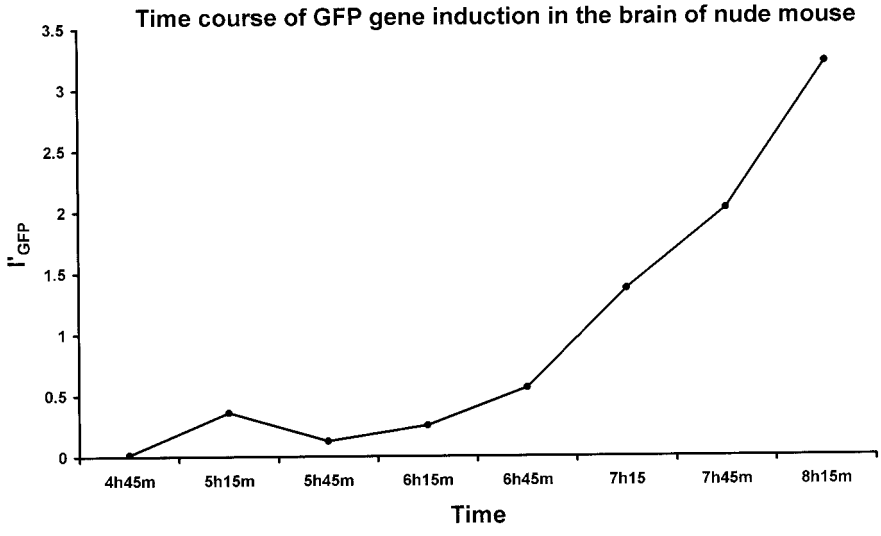

Fig. 3. Time course of GFP gene induction in the brain of a nude mouse. [I'_{GFP}] (see *Materials and Methods*) from a series of whole-body images determined that vAd-GFP expression could be first visualized by 5 h, 15 min after local introduction of vAd-GFP gene in a nude mouse. Increases in expression could be visualized in 30-min intervals.

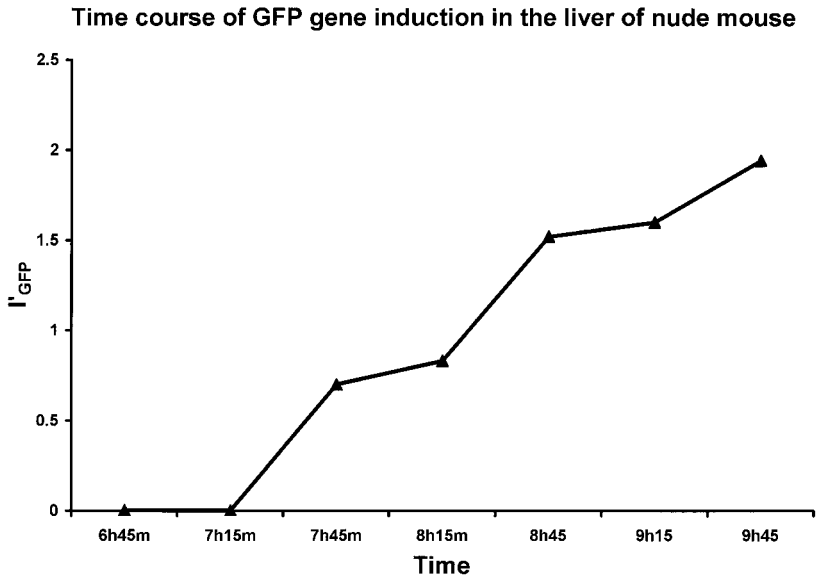

Fig. 4. Time-course GFP gene induction in the liver of a nude mouse. vAd-GFP expression [I'_{GFP}] (see *Materials and Methods*) could be first visualized in the liver by 7 h, 45 min after introduction of vAd-GFP gene in a nude mouse. Increases in expression could be visualized in 30-min intervals.

activated by the gene product (2, 3), a requirement that restricts the type of gene product that can be imaged.

Another approach to noninvasive imaging uses gamma emission from the target region. The techniques, such as micropositron emission tomography and single-photon emission computed tomography (4, 5), require radio-labeled substrates to be localized to some degree by an enzymatic activity of the expressed transgene product. This demanding requirement and the sophisticated equipment for detection and image formation would seem to limit possible applications.

Although animal tissue is rather opaque, optical methods nevertheless offer advantages for noninvasive imaging of transgene expression. Both MRI and radiographic techniques require the expressed gene product to modify either a magnetic field or a diffusion gradient. In contrast, the method described here uses the gene product itself as a source of visible radiation. This radiance is recorded and processed by essentially garden-variety optical instrumentation and image processing. A previous report (6) used the luciferase gene as a reporter for whole-body optical imaging of gene expression. The technique is limited by the need to anesthetize the animals and inject the luciferase substrate. The sensitivity appears inherently low requiring long-term photon acquisition and integration to produce images of immobilized animals (6). Such limits preclude real-time studies and high-throughput *in vivo* screening of gene expression.

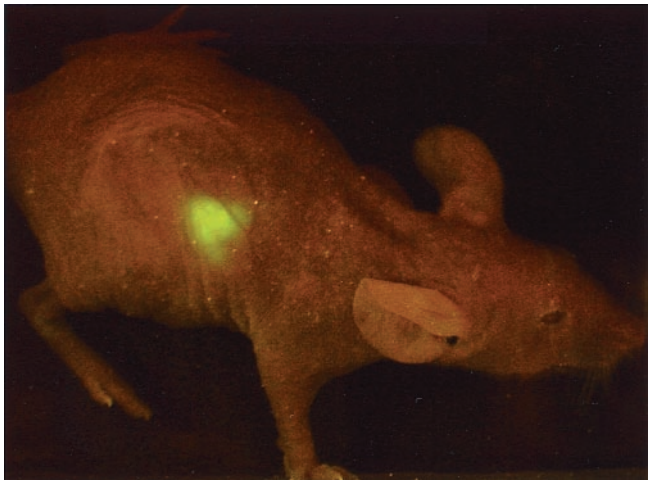

Fig. 5. External whole-body image of vAd-GFP gene expression in the liver. An external image of vAd-GFP gene expression acquired from a nude mouse in the light box 72 h after gene delivery. Lateral, whole-body image of transgene expression in the liver can be clearly visualized through the abdominal wall.

Optical imaging of GFP to map regions of gene expression dispenses with exogenous contrast agents and substrates and offers specificity, sensitivity, simplicity, and real-time recording capability. We previously showed whole-body fluorescence imaging of tumors expressing GFP in living intact animals (7). Other studies have demonstrated superficial imaging of GFP transgene expression in specialized sites such as the skin (8), retina (9), and testis (10). These are unusual in having relatively little tissue between the chromophore and external detector. In the present study, using vAd-GFP as the reporter gene and illumination with a simple light box or fluorescence dissecting microscope, we demonstrate noninvasive, whole-body, real-time fluorescence optical imaging of transgene expression in the major organs of mice including brain, liver, pancreas, prostate, and bone.

vAd-GFP delivered to various organs was induced rapidly and was stable over long time periods, allowing real-time quantitative imaging of transgene expression. These results indicate that gene induction and other kinetic studies can be visualized by whole-body imaging. The high intensity of GFP fluorescence makes transgene expression externally observable from internal organs including brain, liver, pancreas, prostate, and bone (Fig. 1) and presumably in many other organs such as breast, lymph nodes, etc. No contrast agents, radioactive sources, or enzyme substrates need be administered to the animals; only blue light illumination is necessary. The images can be acquired in real time because of the strong GFP signal. The technology reported here can be applied to any gene or promoter fused or operatively linked to GFP in any organ.

We chose vAd-GFP as a vector, because it can transduce many normal tissues efficiently. It was found that vAd-GFP gene is stably expressed in the brain and liver at least for a number of months. Similar studies could be performed in transgenic animals in which GFP or other fluorescent proteins were fused or operatively linked to any gene or promoter.

It is worth noting that the sensitivity and specificity of the method can be greatly increased. Future use of tissue-specific promoters in combination with the ultra-fast lasers (11), dual photon imaging (12), and ballistic photon imaging (13, 14) should offer large gains in specificity, sensitivity, increased depth of detection, and spatial resolution. Visualizing in three dimensions would be possible by using tomographic techniques. This technology provides a powerful *in vivo* tool for noninvasive, real-time visualization of gene expression in living animals. It should facilitate the identification of gene function and development of gene diagnostics and therapeutics.

1. Herschman, H. R., MacLaren, D. C., Iyer, M., Namavari, M., Bobinski, K., Green, L. A., Wu, L., Berk, A. J., Toyokuni, T., Barrio, J. R., *et al*. (2000) *J. Neurosci. Res.* **59,** 699–705.
2. Louie, A. Y., Huber, M. M., Ahrens, E. T., Rothbacher, U., Moats, R., Jacobs, R. E., Fraser, S. E. & Meade, T. J. (2000) *Nat. Biotechnol.* **18,** 321–325.
3. Weissleder, R., Moore, A., Mahmood, U., Bhorade, R., Benveniste, H., Chiocca, E. A. & Basilion, J. P. (2000) *Nat. Med.* **6,** 351–355.
4. Gambhir, S. S., Barrio, J. R., Phelps, M. E., Iyer, M., Namavari, M., Satyamurthy, N., Wu, L., Green, L. A., Bauer, E., MacLaren, D. C., *et al*. (1999) *Proc. Natl. Acad. Sci. USA* **96,** 2333–2338.
5. Tjuvajev, J. G., Finn, R., Watanabe, K., Joshi, R., Oku, T., Kennedy, J., Beattie, B., Koutcher, J., Larson, S. & Blasberg, R. G. (1996) *Cancer Res.* **56,** 4087–4095.
6. Contag, P. R., Olomu, I. N., Stevenson, D. K. & Contag, C. H. (1998) *Nat. Med.* **4,** 245–247.
7. Yang, M., Baranov, E., Jiang, P., Sun, F.-X., Li, X.-M., Li, L., Hasegawa, S., Bouvet, M., Al-Tuwaijri, M., Chishima, T., *et al*. (2000) *Proc. Natl. Acad. Sci. USA* **97,** 1206–1211.
8. Kishimoto, J., Ehama, R., Ge, Y., Kobayashi, T., Nishiyama, T., Detmar, M. & Burgeson, R. E. (2000) *Am. J. Pathol.* **157,** 103–110.
9. Bennett, J., Duan, D., Engelhardt, J. F. & Maguire, A. M. (1997) *Invest. Ophthalmol. Visual Sci.* **38,** 2857–2863.
10. Yamazaki, Y., Yagi, T., Ozaki, T. & Imoto, K. (2000) *J. Exp. Zool.* **286,** 212–218.
11. Alfano, R. R., Demos, S. G. & Gayen, S. K. (1997) *Ann. N.Y. Acad. Sci.* **820,** 248–270.
12. Masters, B. R., So, P. T. & Gratton, E. (1998) *Ann. N.Y. Acad. Sci.* **838,** 58–67.
13. Wu, J., Perelman, L., Dasari, R. & Feld, M. (1997) *Proc. Natl. Acad. Sci. USA* **94,** 8783–8788.
14. Alfano, R. R., Demos, S. G., Galland, P., Gayen, S. K., Guo, Y., Ho, P. P., Liang, X., Liu, F., Wang, L., Wang, Q. Z. & Wang, W. B. (1998) *Ann. N.Y. Acad. Sci.* **838,** 14–28.